CHAPTER 2

The Physical Meaning of Bouguer Anomalies—General Aspects Revisited

Bruno Meurers
University of Vienna, Vienna, Austria

2.1 INTRODUCTION

Interpreting the physical meaning of the Bouguer anomaly is an old problem associated with various assumptions and simplifications made for calculating the height and mass correction terms. It is also related to the purpose the anomaly is used for in different disciplines. For example, for solving the Stokes boundary value problem of physical geodesy we need to know the gravity anomaly at the geoid. In geophysics the goal is finding the gravitational response of subsurface masses on a given reference surface. Ideally, this should be a horizontal plane or a sphere because such reference surfaces simplify processing steps like field continuation or other field transformations applied in the interpretation. But 50 years ago Naudy and Neumann (1965) or Tsuboi (1965) emphasized that the Bouguer anomaly does not represent the gravity effect of anomalous density on a horizontal reference level. Tsuboi (1965) distinguished between station Bouguer anomaly and true Bouguer anomaly, clarifying that the Bouguer gravity is always related to points at the irregular observation surface and not to any other simple reference surface. Nevertheless, even in classical textbooks this fact is not emphasized accordingly (LaFehr, 1991). Another issue in this discussion is the height system used for calculating the normal gravity at a gravity station. Several authors showed that ellipsoidal heights rather than orthometric or normal heights should be used in order to keep a clear concept (e.g., Vogel, 1982; Meurers, 1992). A comprehensive presentation of all problems related to the normal gravity correction has been given by Li and Götze (2001). Hackney and Featherstone (2003) or Vajda et al. (2006) discussed this topic from the perspective of physical geodesy in terms of gravity anomaly and gravity disturbance in order to eliminate the misunderstanding

Understanding the Bouguer Anomaly. DOI: http://dx.doi.org/10.1016/B978-0-12-812913-5.00001-4

between geodesists and geophysicists. Regarding the mass corrections we have to deal with basic assumptions or limitations with respect to density, geometrical approximation of sources, and truncation effects. Hinze et al. (2005) provided a proposal for standard processing of gravity data taking the discussed aspects into account.

The basic assumptions and simplifications in the practical calculation of the Bouguer gravity are closely related to its error budget. The geophysicist has to know these errors for interpreting the anomalies correctly. Using a synthetic concept (e.g., Vogel, 1982) is an appropriate approach to discuss the physical meaning of the Bouguer anomaly and to assess the errors introduced.

Physical geodesy determines the geoid based on observations of gravity $\mathbf{g}$ at the Earth surface. The geoid is closely related to the disturbing potential T leading to the fundamental equation of physical geodesy (Eq. 2.1). It describes the general boundary value problem where Δg is the scalar representation of the gravity anomaly vector $\mathbf{\Delta g}$ in a classical sense with γ denoting the normal gravity vector of the reference ellipsoid:

$$T(P_0) = W(P_0) - U(P_0) \quad \text{disturbing potential}$$

$$\mathbf{\Delta g} = \mathbf{g}(P_0) - \boldsymbol{\gamma}(P_E) \quad \text{gravity anomaly}$$

$$\Delta g = -\left(\frac{\partial T}{\partial n}\right)_{P_0} + \frac{1}{\gamma(P_E)}\left(\frac{\partial \gamma}{\partial n_E}\right)_{P_E} T(P_0) \tag{2.1}$$

Eq. (2.1) results from linearization and combines the derivatives in direction of the plumb lines of the respective gravity field. In geophysics, we are looking for the geometry and the density contrast of anomalous subsurface sources with respect to a reference density model. The definition of the Bouguer anomaly **BA** (Eq. 2.2b) implies using the gravity disturbance vector $\boldsymbol{\delta}\mathbf{g}$ (Eq. 2.2a):

$$\boldsymbol{\delta}\mathbf{g}(P) = \mathbf{g}(P) - \boldsymbol{\gamma}(P) \tag{2.2a}$$

$$\mathbf{BA}(P) = \mathbf{g}(P) - \underbrace{\boldsymbol{\gamma}(P_E)}_{\gamma_0} - \int_{P_E}^{P} \boldsymbol{\Gamma}(\mathbf{s}) \cdot d\mathbf{s} - \mathbf{g}_M(P) = \boldsymbol{\delta}\mathbf{g}(P) - \mathbf{g}_M(P) \tag{2.2b}$$

where $\mathbf{g}_M$ is the gravitational attraction vector caused by all masses above the reference surface including the atmosphere. That is the reason why some authors suggest calling it "topographically corrected gravity disturbance" (e.g., Vajda et al., 2006). $\boldsymbol{\Gamma}$ denotes the gradient tensor of normal gravity, and $d\mathbf{s}$ is an infinitesimally small line element along the plumb line. P_E is the intersection of the plumb line passing P and the ellipsoid. $\gamma(P_E) = \gamma_0$ is the normal gravity on the reference ellipsoid at P_E. Neglecting the deviation of the plumb line from the ellipsoidal normal simplifies Eq. (2.2b):

$$\mathbf{BA}(P) = \mathbf{g}(P) - \underbrace{\gamma(P_E)}_{\gamma_0} - \int_0^{z(P)} \frac{\gamma(z)}{\partial z} dz - \mathbf{g}_M(P) = \delta\mathbf{g}(P) - \mathbf{g}_M(P) \quad (2.2c)$$

where $z(P)$ is the station elevation in the chosen height system and P_E is now the projection of P along the ellipsoid normal (Fig. 2.1). The physical meaning of Eq. (2.2c) depends on the height system applied.

Composing the gravity $\mathbf{g}$ observed at point P on topography synthetically, we have to consider $\mathbf{g}(P)$ as

$$\mathbf{g}(P) = \gamma(P_E) + \int_0^{z=N} \frac{\gamma(z)}{\partial z} dz + \int_{z=N}^{z=N+H} \frac{\gamma(z)}{\partial z} dz + \mathbf{g}_S(P_E) + \int_0^{z=N} \frac{\mathbf{g}_S(z)}{\partial z} dz + \int_{z=N}^{z=N+H} \frac{\mathbf{g}_S(z)}{\partial z} dz + \mathbf{g}_T(P) + \mathbf{g}_G(P) + \mathbf{g}_A(P) \quad (2.3)$$

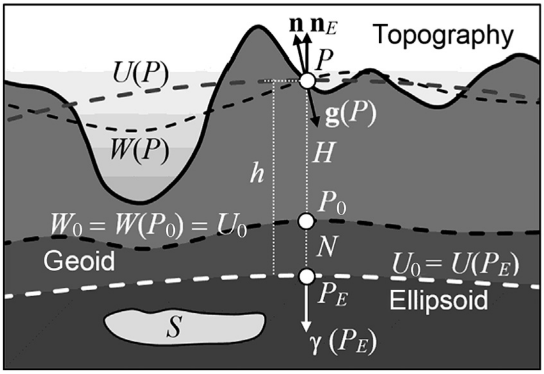

Figure 2.1 Definition of the Bouguer anomaly. Dashed lines show intersections with the equipotential surfaces of the gravity potential W *and the normal gravity potential* U*, respectively. Per definition, the gravity potential* W_0 *on the geoid equals to the normal gravity potential* U_0 *on the reference ellipsoid.* P *marks an observation point at topography. Its projections onto the geoid and the reference ellipsoid are denoted by* P_0 *and* P_E*, respectively.* $\boldsymbol{n}$ *and* $\boldsymbol{n}_E$ *are unit vectors aligned to the surface normal of the corresponding equipotential surfaces.* h *and* H *represent the ellipsoidal and orthometric height, respectively of* P. N *denotes the geoid undulation. The light-gray shaded area S stands exemplarily for all density anomalies inside and outside the ellipsoid.*

The total gravitational attraction vector $\mathbf{g}_M$ is composed of $\mathbf{g}_T$, $\mathbf{g}_G$, and $\mathbf{g}_A$ denoting the contribution of different density domains indicated by the subscripts T (mass between topography and geoid), G (mass between geoid and reference ellipsoid), and A (atmosphere). h describes the ellipsoidal height of P, H its orthometric height, and N the geoid undulation. The latter can be replaced by the normal height and the height anomaly if the normal height system is preferred. $\mathbf{g}_S$ represents the total gravitational attraction vector caused by all anomalous density sources inside and outside the ellipsoid (exemplarily shown by the *light-gray area* S in Fig. 2.1). In this context, anomalous density means the difference between true density and the density distribution of the reference ellipsoid or the model used for mass corrections. From theoretical point of view, we have to consider that the reference ellipsoid does not tell anything about the internal density structure because it is fully defined by only four Stokes' constants. However, Moritz (1990) has shown that structures like those of the preliminary Earth model have a gravity distribution close to the normal gravity. This permits using the normal gravity as a reference. Today there is no need to apply simplified formulae to calculate the normal gravity at the observation site. Either closed formulae including atmospheric correction should be used instead (e.g., Li and Götze, 2001) or second-order Taylor series representations as proposed by Wenzel (1985).

The physical meaning of the Bouguer anomaly is directly visible after inserting Eq. (2.3) into (2.2c), provided ellipsoidal heights are used:

$$\mathbf{BA}(P) = \mathbf{g}_S(P_E) + \int_0^h \frac{\mathbf{g}_S(z)}{\partial z} dz = \mathbf{g}_S(P) \tag{2.4}$$

Contrarily, if orthometric heights are used, we get:

$$\mathbf{BA}(P) = \mathbf{g}_S(P) + \int_0^N \frac{\mathbf{g}_S(z)}{\partial z} dz + \mathbf{g}_G(P) \tag{2.5}$$

which differs from Eq. (2.4) by the geophysical indirect effect (GIE; Hackney and Featherstone, 2003). A similar equation holds true in case of normal heights. Only the Bouguer anomaly evaluated in an ellipsoidal height system is identical with the gravitational attraction vector $\mathbf{g}_S(P)$ of unknown sources. Therefore the ellipsoidal height system should be preferred.

The synthetic concept (Eqs. 2.4 and 2.5) easily permits explaining the gravity effects left in the Bouguer anomaly depending on the basic assumptions made and on the definition of the density domains in Eq. (2.3). It also tells us how to proceed with interpreting the anomaly in the chosen three-dimensional (3D) model space. This even holds if we do not know exactly the density distributions assumed for the mass corrections.

The goal of this chapter is reviewing the problem trying to assess a few specific error sources quantitatively:

- Scalar versus vector representation
- GIE
- Mass correction (truncation effect)
- Normal gravity calculation in areas with negative ellipsoidal heights

2.2 SCALAR VERSUS VECTOR REPRESENTATION

Many interpretation procedures based on the Bouguer anomaly require validity of the Laplace differential equation (LDE). There is no problem as long as the Bouguer anomaly is formulated by a vector equation. Each component of the Bouguer anomaly vector fulfils LDE and therefore is harmonic outside the sources. However, we have rarely access to the full set of vector components. Actually, we observe the norm of a potential gradient vector, which does not meet LDE contrary to its projection onto an arbitrary but constant direction. Therefore we usually deal with scalar quantities resulting from scalar products of the gravity vector **g** and an arbitrary vector **n** as presented in Eq. (2.6).

$$\mathbf{n}(P)\cdot\mathbf{g}_S(P)=\mathbf{n}(P)\cdot\left\{\mathbf{g}(P)-\gamma(P)-\mathbf{g}_M(P)\right\} \tag{2.6}$$

Whether the Bouguer anomaly is a harmonic function or not depends on the choice of **n**. Several options exist as shown in Table 2.1, for example.

Table 2.1 Some Options for Presenting the Bouguer Gravity as a Scalar Quantity

$\mathbf{n}(P)=-\mathbf{r}(P)$	Negative radius vector	$BA(P)$ harmonic	1
$\mathbf{n}(P)=\dfrac{-\mathbf{r}(P)}{\lvert\mathbf{r}(P)\rvert}$	Unit vector along the radial direction	$BA(P)$ nonharmonic	2
$\mathbf{n}(P)=\mathbf{n}_E(P)$	Unit vector along the ellipsoid normal	$BA(P)$ nonharmonic	3
$\mathbf{n}(P)=\mathbf{n}_E=\text{const}$	Unit vector along the ellipsoid normal assumed to be constant everywhere	$BA(P)$ harmonic	4

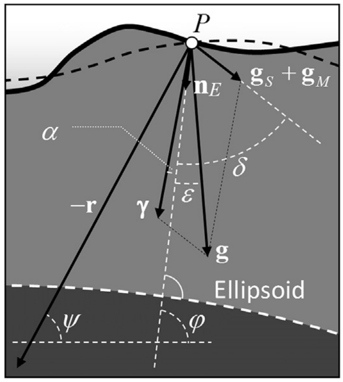

Figure 2.2 Scalar representation of the Bouguer anomaly. $\mathbf{n}_E$ *is the unit vector pointing downward along the ellipsoid normal,* α *the angle between normal gravity vector and ellipsoid normal,* ε *the angle between observed gravity vector* $\mathbf{g}$ *and ellipsoid normal,* δ *the angle between ellipsoid normal and the gravitational attraction vector of all anomalous sources inside the ellipsoid and all mass outside the ellipsoid,* r *the geocentric radius vector,* ψ *geocentric latitude, and* φ *geographic latitude.*

Principally, in all transformations we need to know the direction of the gravity vector $\mathbf{g}$ and not only its norm g as derived from gravity measurements. We can overcome this problem by choosing option 3 leading to a scalar formulation of the Bouguer anomaly (Fig. 2.2):

$$BA(P) = g_S(P)\cos\delta_S(P) = g(P)\cos\varepsilon(P) - \gamma(P)\cos\alpha(P) - g_M(P)\cos\delta_M(P) \tag{2.7}$$

Option 3 is common practice. The ellipsoid normal also defines the orientation of the vertical axis in the Cartesian model space used for the mass correction. This also reduces all modeling efforts because only the vertical component is required for calculating the model response. However the direction of the ellipsoid normal varies from place to place, and therefore the Bouguer anomaly derived from Eq. (2.7) does not strictly fulfill LDE. Option 4 tries to solve the problem by assuming that the ellipsoid normal points to the same direction everywhere in the survey area. This assumption is equivalent to rotating the local coordinate system at each point P such that all vertical axes are aligned, i.e., it neglects the curvature of the Earth's surface. After aligning the vertical axes, the Bouguer anomaly can be regarded as a harmonic function in planar approximation. However, it is important to keep in mind that this approximation causes errors which have to be considered in field continuation, e.g., for high accurate 3D interpolation as well as in 3D modeling. Moreover, this concept fails for

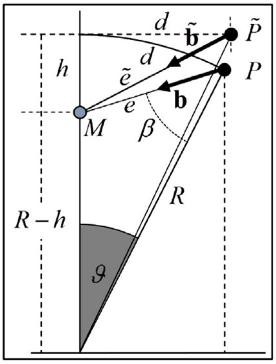

Figure 2.3 Effect of bending the Earth's surface into a horizontal plane.

large-scale investigations. Modern 3D modeling codes (e.g., Götze, 1984, http://potentialgs.com/) are able to get rid of the problem by taking the curvature into account.

We can roughly estimate the magnitude of the error. Option 4 is equivalent to bending the Earth's surface into a horizontal plane by shifting the observation point P to $\tilde{P}$ (see Fig. 2.3). Let $\mathbf{b}$ and $\tilde{\mathbf{b}}$ be the gravitational attraction vector at the observation point P and $\tilde{P}$, respectively, caused by a point source with mass M located in the depth h below the Earth's surface. According to Eq. (2.7) the Bouguer anomaly BA at a point P then reads in spherical approximation as

$$\begin{aligned} BA(P) &= \frac{GM}{e^2}\cos\beta = \frac{GM}{e^2}\frac{1}{e}\sqrt{e^2-(R-h)^2\sin^2\vartheta} \\ BA(\tilde{P}) &= \frac{GM}{\tilde{e}^2}\frac{h}{\tilde{e}} \end{aligned} \tag{2.8}$$

with

$$e=\sqrt{R^2+(R-h)^2-2R(R-h)\cos\vartheta} \quad d=R\vartheta$$
$$\tilde{e}=\sqrt{R^2\vartheta^2+h^2}$$
$$\sin\beta=\frac{R-h}{e}\sin\vartheta \quad \cos\beta=\frac{1}{e}\sqrt{e^2-(R-h)^2\sin^2\vartheta}$$

R is the Earth's radius and ϑ the angle between the position vectors of M and P. The difference between the Bouguer anomalies at P and

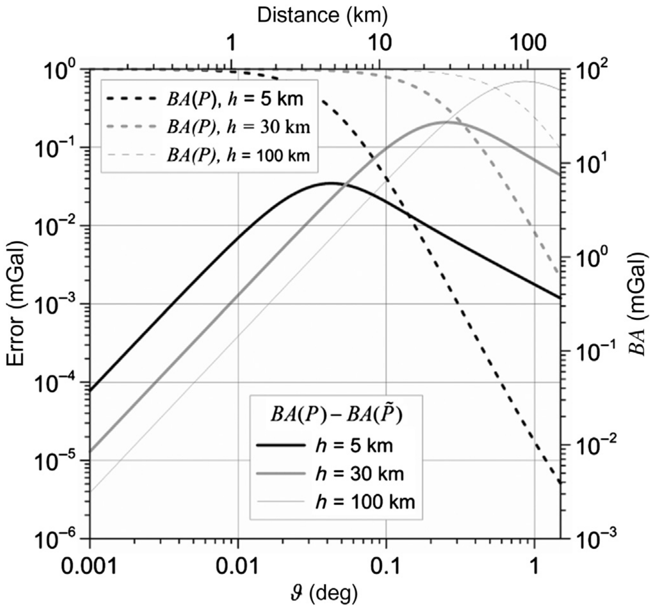

Figure 2.4 Error caused by neglecting the curvature of the Earth's surface (refer to Fig. 2.3 and Eq. 2.8).

$\tilde{P}$ depends on ϑ and h. For a mass causing an anomaly of 100 mGal (1 mGal = 10^{-5} m/s^2) at a surface point with $\vartheta = 0$ the error can grow up to 1 mGal or 1% in this simple case (see Fig. 2.4).

Inherently, options 3 and 4 ignore the misalignment between the ellipsoid normal and the direction of the observed gravity vector. The error introduced by neglecting the misalignment of **g** and γ can be estimated easily. Close to the Earth's surface, the angle α between the true direction of the normal gravity vector at P and the ellipsoid normal passing P is very small. Ignoring α we get (see Fig. 2.2)

$$g = |\mathbf{g}| = \sqrt{g_{s,1}^2 + g_{s,2}^2 + (\gamma_3 + g_{s,3})^2} = (\gamma_3 + g_{s,3})\sqrt{\underbrace{\frac{g_{s,1}^2 + g_{s,2}^2}{(\gamma_3 + g_{s,3})^2}}_{\mathrm{tg}^2\,\varepsilon \ll 1} + 1}$$

$$\Rightarrow \quad g_{s,3} \cong g - \gamma$$

where the indices reflect the components of the gravitational attraction vector $\mathbf{g}_s$ of the anomalous sources in the local Cartesian coordinate

Table 2.2 Error Caused by Ignoring the Misalignment Between g and γ

ε ($''$)	Error (nms^{-2})	
10	11	Flat terrain
30	104	Mountainous area
60	415	Maximum estimate

system. ε corresponds to the deflection from the vertical in good approximation. Again, $g_{s,3}$ fulfills LDE in contrast to $|\mathbf{g}_s|$, that means, $BA(P)$ is harmonic. Table 2.2 represents error estimates for typical terrain scenarios.

2.3 THE GEOPHYSICAL INDIRECT EFFECT

For the first time, Meurers and Ruess (2009) calculated the Bouguer anomaly for Austria based on ellipsoidal heights derived from a precise geoid model (Pail et al., 2008), assuming a crustal density of 2670 kg/m^3 both for topography and the space between geoid and ellipsoid. The GIE is the difference between this product and the Bouguer anomaly based on orthometric heights. The GIE estimate for the Eastern Alps shows that ignoring the GIE induces an offset and, in addition, height dependent error components (Fig. 2.5).

Due to the dominating long-wavelength character of the geoid undulation the observed GIE–geoid admittance reflects on average the Bouguer gradient of -0.196 mGal/m in agreement with the estimate, e.g., by Hinze et al. (2005). In addition, Fig. 2.5C and D reveals small-amplitude signatures of the GIE, which are related to the local topography imaged in the high frequency part of the geoid undulation. Due to the latter, the GIE can vary locally by 0.1 mGal with a topographic height difference of 1 km, which is negligible in most studies. Therefore for small-scale surveys the GIE is less important. However, estimates of the isostatic state of a region will suffer from the offset directly influencing the average of isostatic anomalies.

Contrarily, the GIE is critical for large-scale investigations. Fig. 2.6 shows the expected effects for Europe based on the EGG2008 quasigeoid (Denker, 2009, http://www.isgeoid.polimi.it/Geoid/Europe/europe2008_g.html).

Ignoring the GIE will deteriorate 3D interpretation of deep sources like the lithosphere–asthenosphere boundary (LAB). Assuming a

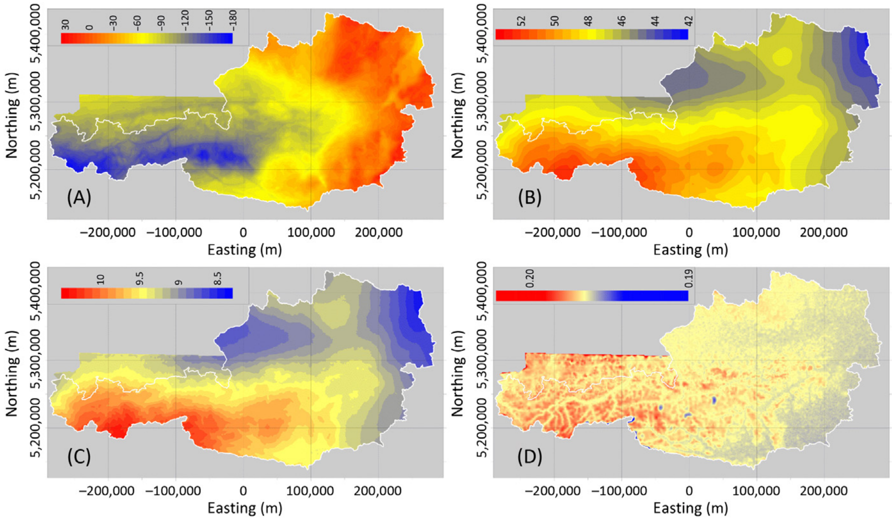

Figure 2.5 Bouguer anomaly, geoid, GIE, and GIE−geoid admittance of Austria. (A) Bouguer anomaly (mGal) based on ellipsoidal heights (Meurers and Ruess, 2009), (B) geoid (m) (Pail et al., 2008), (C) geophysical indirect effect (mGal) assuming a crustal density of 2670 kg/m^3, (D) GIE−geoid admittance (mGal/m). Gauss−Krüger coordinate system centered at 13°20′ E.

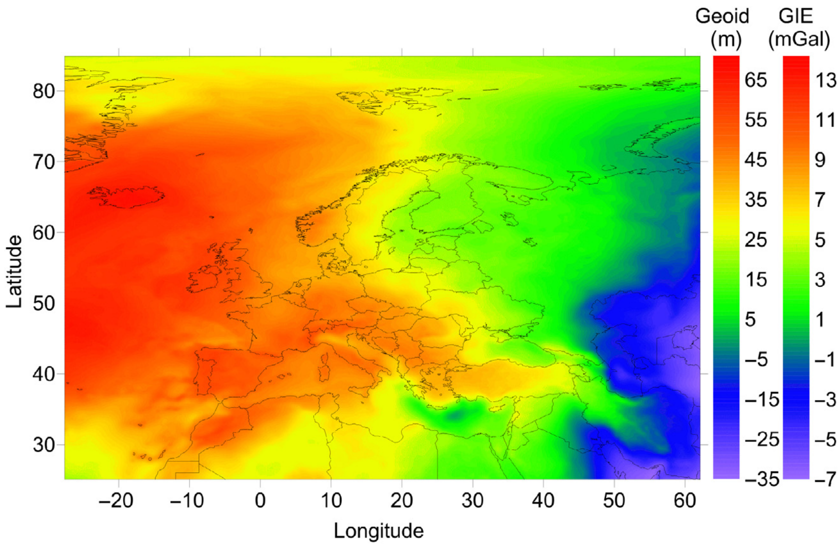

Figure 2.6 EGG2008 quasigeoid (http://www.isgeoid.polimi.it/Geoid/Europe/europe2008_g.html, Denker, 2009) and its corresponding GIE estimate in Europe based on an average GIE−geoid admittance of 0.196 mGal/m.

density contrast $\delta\rho_{LAB}$ of 50 kg/m^3 at the LAB, the GIE can be expressed as depth variation of the LAB interface:

$$GIE = \delta g_{LAB} \cong 2\pi G \delta\rho_{LAB} \delta h_{LAB} \Rightarrow$$
$$\delta h_{LAB}[\mathrm{km}] \cong \frac{GIE[\mathrm{mGal}]}{2} \text{ with } \delta\rho_{LAB} = 50 \ \mathrm{kg/m^3} \tag{2.9}$$

The corresponding total LAB interface error would be 10 km approximately.

2.4 TRUNCATION ERROR OF THE MASS CORRECTION

The mass correction term in Eq. (2.2c) implicitly considers both solid rocks within topography and water (lakes, ocean, and ice) with different densities. In principle, the mass correction has to be performed over the entire Earth surface. Just by convention, it is truncated beyond the outer limit of the Hayford zone O_2 corresponding to an angular distance of roughly 1.5 degrees or 167 km. Because Eq. (2.2c) requires removing all topographic masses globally, this violates the synthetic concept and may induce a bias as well as small height-dependent errors.

Fig. 2.7 shows the effect of extending the mass correction boundary from 167 to 217 km for the Alpine area in Western Austria. Besides a bias, the differences are clearly correlated with the station elevations.

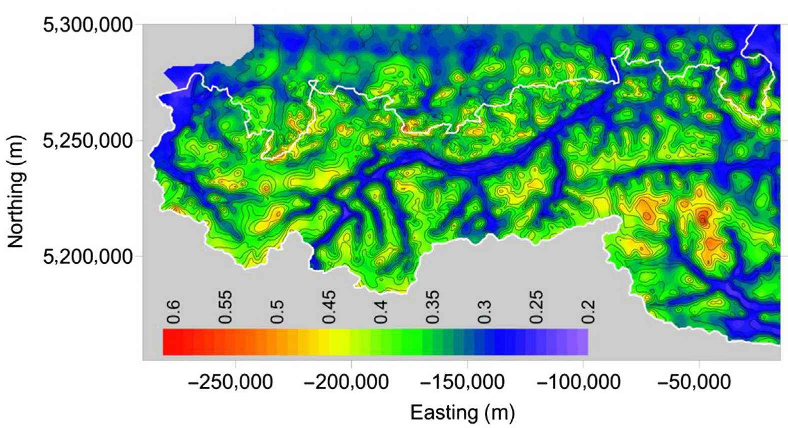

Figure 2.7 Effect of extending the mass correction boundary from 167 to 217 km for the Alpine area in Western Austria. Colors indicate the difference in mGal. Contour lines show the station elevation in 250 m intervals. Gauss–Krüger coordinate system centered at 13°20′E.

Mikuška et al. (2006a,b, 2008) studied the truncation effect in detail. They estimated the gravitational effect of both the distant terrain masses and the bathymetric relief located globally beyond the Hayford zone O_2 in spherical approximation and called it "distant relief effect" (DRE).

The distant masses turned out to produce large gravity effects globally ranging between −60 and −210 mGal with horizontal gradients up to 0.03 mGal/km and vertical gradients up to 3 mGal/km. Mikuška et al. (2006a) recommended considering the effect of distant masses for large-scale investigations or even for detailed surveys given the station heights vary remarkably. In the Alpine region, the gravity effect of the distant masses is well described by an E-W trend of 0.005 mGal/km and a bias of 105 mGal (Mikuška et al., 2006b).

In the sense of Eq. (2.2c) the real earth can be regarded (e.g., Meurers and Vajda, 2006) as synthetically composed of

- the mass of the reference ellipsoid,
- topographic surplus mass (outside the reference ellipsoid),
- water (ice) (inside or outside the reference ellipsoid),
- topographic deficit mass (inside the reference ellipsoid), and
- mass anomalies inside the reference ellipsoid.

The gravity of the reference ellipsoid is just the normal gravity used in Eq. (2.2c). The total mass of the real earth must be equal to the mass of the reference ellipsoid, because the solid spherical harmonic expansions of their gravitational potentials have identical zero-degree terms. Therefore the topographic surplus mass, the deficit mass, and all water must be balanced by the density anomalies inside the reference ellipsoid. Consequently, the Bouguer anomaly defined in Eq. (2.2c) does not only contain the signal of local sources but also the signal of all compensating mass, i.e., the 3D model space has to cover the entire Earth. The limitation of the 3D model space to smaller scales is possible as long as the gravity effect of all distant sources is smooth within the survey area and thus can be removed by trend field separation.

From this point of view, it is questionable, whether the DRE should be corrected for or not, and the issue is still under debate. The gravity effect of solid topographic mass and ocean water is isostatically compensated to a high extent by the crust-mantle boundary undulation (root and antiroot). It is reasonable to expect that the compensating masses produce similar horizontal and vertical gradients as the DRE does. If the DRE is removed then an isostatic correction should be applied as well as done in crustal balancing investigations based on isostatic anomalies. This idea has been proposed already by Hinze et al. (2005). However, crustal as well as large subcrustal mantle density variations take part in the isostatic compensation (Kaban et al., 2004). The amplitude of isostatic anomalies based on ideal isostatic models like Airy or Vening-Meinesz is significantly reduced when using real lithosphere data (Kaban et al., 1999). Therefore even the classical isostatic correction would not remove totally the gravity effect of all the mass inhomogeneity down to the upper mantle taking part in topography compensation.

It always depends on the problem we are faced to, which distant sources have to be corrected for. As mentioned earlier, in most cases 3D modeling requires a priori trend separation for keeping the 3D model space as small as possible. The horizontal DRE gradient varies very smoothly, and therefore the trend removed by the applied filter procedures includes the DRE trend too. Truncation is justified as long as it does not cause height-dependent errors. Therefore the vertical DRE gradient is more critical especially in rugged terrain because in these regions the DRE induces station height-dependent terms that cannot be eliminated by smooth trend functions. In the area of the Alps the DRE vertical gradient is about 0.5 mGal/km (Mikuška et al., 2006a,b). Elevation differences in the close surrounding of valleys amounts up to 2 km producing an anomaly of 1 mGal, which is closely correlated with topography and affects sedimentary filling estimates systematically.

2.5 NORMAL GRAVITY CALCULATION IN AREAS WITH NEGATIVE ELLIPSOIDAL HEIGHTS

Orthometric or normal heights are positive almost everywhere on the Earth surface. This allows applying closed expressions (Hofmann-Wellenhof and Moritz, 2005; Li and Götze, 2001) or series expansions (Wenzel, 1985) for the normal gravity calculation almost worldwide. This does not hold true for wide areas if ellipsoidal heights are used. Ellipsoidal heights are negative not only in some oceanic regions, but also onshore along the coast (Fig. 2.8).

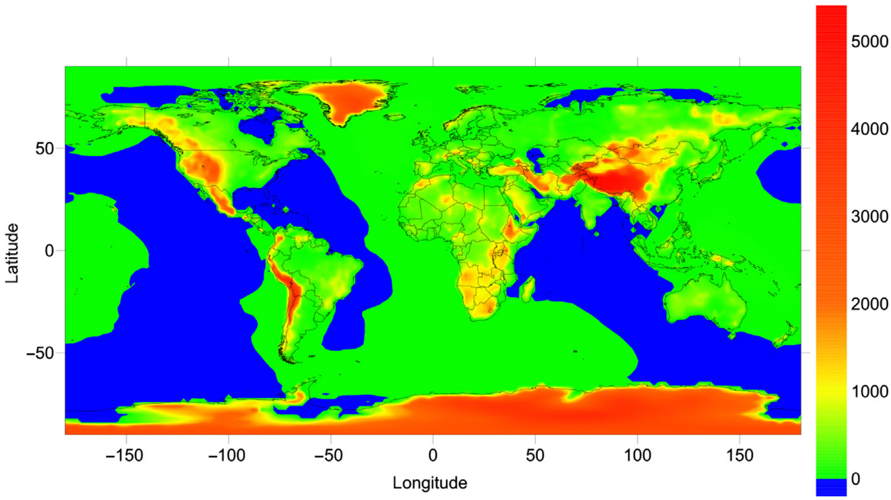

Figure 2.8 Global ellipsoidal heights (m) derived from GTOPO30 (http://www.temis.nl/data/topo/dem2grid.html) and the EGM2008 geoid undulations (Pavlis et al., 2012). Areas below the reference ellipsoid are displayed in blue.

Because the normal potential is uniquely defined by four Stokes' constants (e.g., Hofmann-Wellenhof and Moritz, 2005), no assumption is required regarding the internal mass distribution of the reference ellipsoid. Due to the nonuniqueness principle of potential theory, infinitely many internal mass distributions are able to produce the normal potential. The expansion of the normal potential into solid spherical harmonics converges down to a sphere closely surrounding the focal points of the reference ellipsoid (Moritz, 1980). According to the equivalent source principle a surface density distribution spread over the sphere of convergence exists that causes the normal potential. Thus the normal potential is harmonic far below the surface of the reference ellipsoid. However, this concept valid in physical geodesy is not suitable in geophysics because the link to the model space is missing. Normal potential is assumed to be caused by a suitable density stratification (spheroidal, ellipsoidal) within the reference ellipsoid, which serves as reference density in 3D modeling. Within the ellipsoid Poisson's differential equation holds rather than LDE because the disturbing potential is not harmonic below the reference ellipsoid surface. Taylor series approximation of normal gravity or closed expressions are no longer applicable.

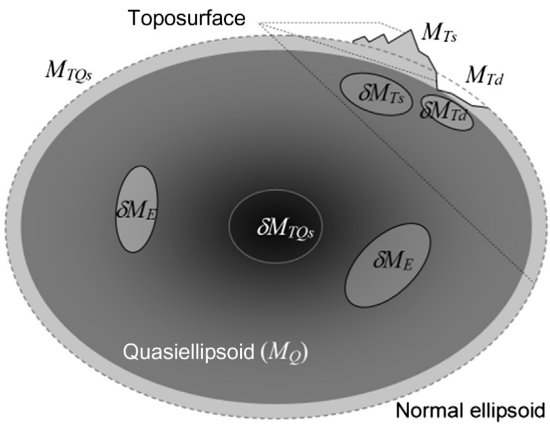

Figure 2.9 Quasiellipsoid concept (Vajda et al., 2004; Meurers and Vajda, 2006). For explanation, see text.

Therefore the common way of normal gravity determination is not possible or induces systematic errors. We need alternate reference Earth models. Vajda et al. (2004) suggest referring to a so-called quasiellipsoid. Alternatively, we can make use of ellipsoidal models presenting normal gravity at their surface (Karcol, 2011), see also Chapter 4, Normal Earth Gravity Field Versus Gravity Effect of Layered Ellipsoidal Model.

The quasiellipsoid (Fig. 2.9) is defined as a spheroid located inside the reference ellipsoid with constant distance between each surface point and its projection onto the reference ellipsoid along the reference ellipsoidal normal. Each point of the real toposurface is either on or outside the quasiellipsoid (Vajda et al., 2004). The internal mass density distribution is such that its external gravity field equals exactly to that of the reference ellipsoid. Outside the reference ellipsoid the potential field is uniquely determined by the normal gravity on the reference ellipsoid. Within the space between the reference ellipsoid and the quasiellipsoid LDE holds allowing for analytical continuation of the external potential down to the surface of the quasiellipsoid. Hence, everywhere outside and on the quasiellipsoid, the closed expressions or series expansions for the normal gravity can be applied, i.e., the components of the Bouguer gravity disturbance vector can now be calculated without an a priori knowledge of the internal density structure even at points with negative ellipsoidal heights.

The quasiellipsoid has the same total mass as the reference ellipsoid. Therefore additional anomalous mass δM_{TQs} exists in its interior that balances the mass M_{TQs} between reference and quasiellipsoid as well as the topographic surplus M_{Ts} and deficit M_{Td} mass. However, this leads to a small global- and height-dependent gravity signal (Meurers and Vajda, 2006). The Bouguer anomalies differ in both concepts by one constant- and one height-dependent term which can be estimated in spherical approximation as:

$$\delta g \approx -4\pi G\rho h'\left(1 - 2\frac{h}{R_0}\right) \tag{2.10}$$

where h' denotes the radius difference between ellipsoid and quasiellipsoid while R_0 is the radius of the reference ellipsoid. Assuming a crustal density of 2670 kg/m^3 and $h' = 0.1$ km the height dependence is estimated to be 70 nm/s^2 per km.

2.6 CONCLUSION

Only the Bouguer anomaly based on ellipsoidal heights corresponds exactly to the gravity effect of all masses below the toposurface that differ from the density of the reference Earth (if located within the reference ellipsoid) and constant density, respectively (if located outside the reference ellipsoid) at the observation point. At local and regional scales the Bouguer gravity can be regarded to be harmonic in planar approximation everywhere above and on the toposurface. The scalar representation is justified but can be associated with considerable errors at larger scales. The GIE may interfere with signals of deep (upper mantle) sources and therefore ellipsoidal heights should be used for calculating the Bouguer anomaly in large-scale studies. The truncation of the mass correction area is justified only for local- to regional-scale investigations. However the DRE is important on large scales and even sometimes at regional scales at specific locations. If applied a global isostatic correction should be considered as well to account for subsurface masses compensating the topographic load. The normal gravity cannot be calculated by applying the classical concepts in areas with negative ellipsoidal heights. We need either the quasiellipsoid approach or a global Earth model with spheroidal density stratification. In the quasiellipsoid approach the density distribution of the reference ellipsoid does not need to be known. However a global- and height-dependent signal is left in the Bouguer anomaly.

REFERENCES

Denker, H., 2009. The European Gravimetric Quasigeoid EGG2008. Eos Trans. AGU, 90(22), Jt. Assem. Suppl., Abstract CG73A-03.

Götze, H.J., 1984. Über den Einsatz interaktiver Computergraphik im Rahmen 3-dimensionaler Interpretationstechniken in Gravimetrie und Magnetik. Habilitationsschrift. Technische Universität Clausthal, Clausthal.

Hackney, R.I., Featherstone, W.E., 2003. Geodetic versus geophysical perspectives of the 'gravity anomaly'. Geophys. J. Int. 154, 35–43.

Hinze, W.J., Aiken, C., Brozena, J., Coakley, B., Dater, D., Flanagan, G., et al., 2005. New standards for reducing gravity data: the North American gravity database. Geophysics 70 (4), J25–J32.

Hofmann-Wellenhof, B., Moritz, H., 2005. Physical Geodesy. Springer, Vienna and New York, NY, 403 p.

Kaban, M.K., Schwintzer, P., Tikhotsky, S.A., 1999. Global isostatic gravity model of the Earth. Geophys. J. Int. 136, 519–536.

Kaban, M.K., Schwintzer, P., Reigber, Ch, 2004. A new isostatic model of the lithosphere and gravity field. J. Geodesy 78, 368–385. Available from: http://dx.doi.org/10.1007/s00190-004-0401-6.

Karcol, R., 2011. Gravitational attraction and potential of spherical shell with radially dependent density. Stud. Geophys. Geod. 55 (1), 21–34.

LaFehr, T.R., 1991. Standardization in gravity reduction. Geophysics 56, 1170–1178.

Li, X., Götze, H.J., 2001. Ellipsoid, geoid, gravity, geodesy, and geophysics. Geophysics 66, 1660–1668.

Meurers, B., 1992. Untersuchungen zur Bestimmung und Analyse des Schwerefeldes im Hochgebirge am Beispiel der Ostalpen. Österr. Beitr. Met. Geoph. 6, 146 S.

Meurers, B., Ruess, D., 2009. A new Bouguer gravity map of Austria. Aust. J. Earth Sci. 102, 62–70.

Meurers, B., Vajda, P., 2006. Some aspects of Bouguer gravity determination - revisited. In: Contributions to Geophysics and Geodesy, Vol. 36, Special Issue: 2nd Workshop on International Gravity Field Research, Smolenice 2006, 99–112.

Mikuška, J., Pašteka, R., Marušiak, I., 2006a. Estimation of distant relief effect in gravimetry. Geophysics 71, J59–J69.

Mikuška, J., Pašteka, R., Marušiak, I., Bielik, M., Hajach, M., 2006b. Distant relief effect and its possible impact on large-scale gravity interpretations. In: EAGE 68th Conference & Exhibition—Vienna, Austria, 12–15 June 2006, extended abstract H017, Available from: http://dx.doi.org/10.3997/2214-4609.201402092.

Mikuška, J., Pašteka, R., Mrlina, J., Marušiak, I., 2008. Gravitational effect of distant Earth relief within the territory of former Czechoslovakia. Stud. Geophys. Geod. 52, 381–396.

Moritz, H., 1980. Advanced Physical Geodesy. Herbert Wichmann Verlag, Karlsruhe.

Moritz, H., 1990. The Figure of the Earth. Herbert Wichmann Verlag, Karlsruhe.

Naudy, H., Neumann, R., 1965. Sur la definition de l'anomalie de Bouguer et ses consequences practique, Geophys. Prospect., 13. pp. 1–11.

Pail, R., Kühtreiber, N., Wiesenhofer, B., Hofmann-Wellenhof, B., Of, G., Steinbach, O., et al., 2008. The Austrian Geoid 2007. Vgi - Österreichische Zeitschrift für Vermessung und Geoinformation 96 (1), 3–14, Österreichische Gesellschaft für Vermessung und Geoinformation (OVG), ISSN 0029-9650.

Pavlis, N.K., Holmes, S.A., Kenyon, S.C., Factor, J.K., 2012. The development and evaluation of the Earth Gravitational Model 2008 (EGM2008). J. Geophys. Res. 117, B04406. Available from: http://dx.doi.org/10.1029/2011JB008916.

Tsuboi, C., 1965. Calculations of Bouguer anomalies with due regard the anomaly in the vertical gradient. Proc. Jap. Acad. Sci. 41, 386−391.

Vajda, P., Vaníček, P., Meurers, B., 2006. A new physical foundation for anomalous gravity. Stud. Geophys. Geodesy 50 (2), 189−216. Available from: http://dx.doi.org/10.1007/s11200-006-0012-1.

Vajda, P., Vaníček, P., Novák, P., Meurers, B., 2004. On evaluation of Newton integrals in geodetic coordinates: exact formulation and spherical approximation. Contrib. Geophys. Geodesy 34, 289−314.

Vogel, A., 1982. Synthesis instead of reductions—new approaches to gravity interpretations, Earth Evolution Sciences, 2. Vieweg, Braunschweig, pp. 117−120.

Wenzel, F., 1985. Hochauflösende Kugelfunktionsmodelle für das Gravitationspotential der Erde. Wiss. Arb. Fachr. Vermessungswesen Univ, Hannover, p. 137.